

# Multispectral MRI image segmentation using Markov random field model

Ali Ahmadvand · Peyman Kabiri

Received: 12 February 2014 / Revised: 23 November 2014 / Accepted: 28 November 2014 / Published online: 6 December 2014  
© Springer-Verlag London 2014

**Abstract** Magnetic resonance imaging (MRI) is used to capture images in different modalities such as *T1-weighted*, *T2-weighted*, and *PD-weighted*. This paper proposes a new method for the fusion of different channels in MRI image segmentation. In the reported work, a new feature vector for multispectral MRI brain segmentation is proposed. Fuzzy C-means clustering method is applied on the three different extracted feature vectors, and results are reported. Experimental results show that the proposed feature vector presents good noise immunity. Paper reports a new segmentation method based on Markov random field and the proposed feature vector to combine spatial and spectral information for MRI image segmentation. The proposed method was applied on the BrainWeb MRI image dataset with added noise, and the segmentation results are reported and compared with some known reported works.

**Keywords** *T1-weighted* · *T2-weighted* · *PD-weighted* · Segmentation · FCM method · MRF method

## 1 Introduction

Magnetic resonance imaging (MRI) is a powerful and popular tool for medical imaging. MRI is used in different treatment procedures such as diagnosis and follow-up. MRI is an effective diagnostic tool in many medical treatments, in

which, image segmentation plays an important role [1]. Manual segmentation of brain is often time-consuming; therefore, automatic segmentation can be used to speedup the process. MRI images from brain are segmented into three classes such as gray matter (GM), white matter (WM), and cerebrospinal fluid (CSF) [2]. Structure of the human brain is very deformable and has complex boundaries between different regions.

Moreover, MRI images have common artifacts such as partial volume effect (PVE) and intensity non-uniformity (INU) that are resulted during the imaging process. In MRI imaging, each voxel represents a combination of different types of tissues within a 3D block of a brain slice. PVE is a representation of the complexity of the combination of different types of tissues within a voxel. High PVE in MRI imaging makes the image segmentation more difficult. INU is caused due to the limitations in hardware and degrades the quality of acquired MRI images [3,4].

Finite mixture model (FMM) is commonly used for MRI brain segmentation. Greenspan et al. [5] proposed constrained Gaussian mixture model (CGMM) for MRI image segmentation where a large number of Gaussian models are used to model each tissue. Tohka et al. [6] used real-coded genetic algorithm (RCGA) to estimate mixture parameters for MRI image segmentation. Expectation maximization (EM) algorithm is used for parameter approximation. However, this method has a high computational cost and can fall into local maxima. In another reported work, Tohka et al. [7] proposed a combination of EM and GA algorithms to estimate parameters for MRI image segmentation.

In image segmentation problem areas, such as, remote sensing and MRI medical imaging, Markov random field (MRF) is reportedly used for the fusion of spectral, spatial, and contextual properties [8,9]. Van Leemput et al. [9] proposed one of the first and most reliable methods for MRI

---

A. Ahmadvand · P. Kabiri (✉)  
School of Computer Engineering, Iran University of Science and Technology, University Road, Hengam Street, Resalat Square, Narmak, 16846-13114 Tehran, Iran  
e-mail: Peyman.Kabiri@iust.ac.ir

A. Ahmadvand  
e-mail: ali.ahmadvand.66@gmail.com

brain segmentation called Koen Van Leemput (KVL), which is based on MRF algorithm. KVL uses EM algorithm for parameter approximation. The conventional MRF uses EM and simulated annealing methods both with high computational costs [2, 10]. Yousefi et al. [2] used a combination of ant colony optimization (ACO) algorithm and gossiping algorithm for the optimization stage in the MRF model. Sahar et al. claim that the reported algorithm outperforms the conventional MRF-simulated annealing and MRF-ACO algorithms and can operate in real time. In another reported work, a combination of MRF and a typical clustering method mainly was used to increase the robustness of the clustering method against noise [11]. Rajapakse et al. [12] used Gaussian mixture model (GMM) for brain segmentation. In their work, MRF model was used to improve the segmentation result. Marroquín et al. [13] proposed another method for MRI brain segmentation. This algorithm uses maximum a posteriori (MAP) estimator and maximization of the posterior marginals (MPM) estimator where a variant of EM algorithm for robust approximation of MAP is defined for MRF. This algorithm is called MPM-MAP. Zhang et al. [14] proposed another related method based on hidden Markov random field (HMRF) model that uses EM algorithm to fit the HMRF parameters and is called EM-HMRF.

Different extensions of fuzzy C-means (FCM) algorithm are proposed for MRI brain image segmentation [15, 16]. Rivest-Hénault and Cheriet [17] proposed a level set method for MRI brain segmentation. Level set method needs good initialization to prevent it from falling into local minima. They used FCM for the initialization and then applied level set method to improve the results. Wu et al. [18] proposed a method to combine support vector machine (SVM) and MRF methods for MRI image segmentation. They proposed a new energy function for MRF method based on SVM classification. Their proposed method suffers from high execution time for the training and validation of the results.

Atlas-based methods are active research areas in MRI image segmentation. Atlas-based methods use different pre-labeled images and prior anatomical information for brain segmentation. These methods consist of three main steps such as registration, label propagation, and final segmentation. Atlas-based methods are also proposed for brain segmentation [19].

This paper proposes a new feature vector for multispectral MRI image segmentation with high noise immunity. The use of *T1-weighted* image for MRI image segmentation of the brain is well studied. Images, such as *T2-weighted* and *Proton Density-weighted (PD-weighted)* that are produced by MRI, can be used as additional information to increase the segmentation accuracy. In the proposed approach, using the three aforementioned MRI imagery products, a wavelet-based method is applied to extract a feature vector. The extracted feature vector is named modality fusion vector

(MFV). Later on, the MFV is used in FCM and a combination of FCM and MRF methods (FCMRF) for segmentation. In the reported work, BrainWeb dataset is used for the experiments.

## 2 Discrete wavelet transform

Discrete wavelet transform (DWT) is mathematical model for multi-resolution analysis. Wavelet transform is a common method for spatial frequency analysis. 1D continuous wavelet transform (CWT) is represented by Eq. 1.

$$CW(a, b) = \frac{1}{\sqrt{a}} \int y(t) \varphi\left(\frac{t-b}{a}\right) dt \quad (1)$$

where  $y(t)$  is the input signal,  $\varphi$  is the wavelet function. Parameters  $a$  and  $b$  are scaling and translation parameters, respectively. The base functions of a DWT are captured by means of sampling from CWT.  $\varphi_{j,k}(t)$  function is presented in Eq. 2.

$$\varphi_{j,k}(t) = 2^{-n/2} \varphi(2^{-n}t - m), m, n \in N \quad (2)$$

2D DWT is derived from 1D wavelet transform by applying filters in rows and columns. 2D DWT divides the images into four different sub-bands i.e., *LL*, *LH*, *HL* and *HH*. Each sub-band can represent an image and they approximate vertical, horizontal, diagonal details, respectively.

## 3 Proposed method

This section presents a method for multispectral MRI image segmentation. In the first stage, a wavelet-based data fusion method is proposed and MFV is extracted. In the second stage, MFV and two different feature vectors are applied on FCM and different label fields are produced. The result shows that MFV has high noise immunity compared with other feature vectors. In the third stage, the feature vector extracted from *T1-weighted* image is used for the initial segmentation. Later on, a MFV-based energy function for the MRF optimization is proposed that is called extended FCMRF (E-FCMRF). This energy function uses MFV-based label field to incorporate the spectral features in segmentation of MRI image. This energy function is compared against another energy function that uses *T2-weighted* and *PD-weighted* label field to incorporate the spectral features in segmentation and results are reported.

### 3.1 Modality fusion vector extraction

The MFV is extracted from the fusion of three *T1-weighted*, *T2-weighted* and *PD-weighted* images. Wavelet analysis is used for data fusion and extraction of the MFV. *T1-weighted*

images have higher resolution than *T2-weighted* and *PD-weighted* images. Therefore, these images are more detailed than other spectral images. This is why in many reported works only *T1-weighted* images are used for MRI brain image segmentation. This paper proposes fusion of different modalities to improve segmentation accuracy for MRI brain images in high level of noise. Construction of MFV includes two stages. Initially, different image modalities are divided into four different channels such as Low horizontal and low vertical (*LL*) and the detailed images consist of high horizontal and low vertical (*HL*), low horizontal and high vertical (*LH*), and high horizontal and high vertical (*HH*) frequencies. In the second stage, *T2-weighted* and *PD-weighted* images are used to produce an approximated image. Wavelet fusion method [20,21] is described in Fig. 1. Multispectral MRI images are not taken simultaneously like different multispectral images such as in remote sensing applications. Therefore, different modalities need a registration step to geometrically match the channels. Wavelet fusion can be applied to Brain-Web dataset due to the registration of different channels in this dataset. Otherwise for datasets that are not registered, the registration of different channels is needed.

Approximation image is made by weighted averaging of *T2-weighted* and *PD-weighted* images. Detailed images are also produced using weighted averaging of *T1-weighted* and *T2-weighted* images. The calculation method is presented in Eqs. 3 and 4.

$$APP\_img = 0.5 \times App(T2\_weighted) + App(PD\_weighted) \tag{3}$$

$$Detail\_img = 0.5 \times Detail(T1\_weighted) + Detail(T2\_weighted) \tag{4}$$

*F1* is a one-dimensional feature vector and only *T1-weighted* image is used for segmentation. *F2* is a three-dimensional feature vector. *F1* and *F2* are presented in Eqs. 5 and 6, respectively.

$$F1 = [T1\_weighted(i, j)]^T \tag{5}$$

$$F2 = \begin{bmatrix} T1\_weighted(i, j) \\ T2\_weighted(i, j) \\ PD\_weighted(i, j) \end{bmatrix} \tag{6}$$

*i, j* are voxels location in image. MFV is a two-dimensional feature vector. MFV improves the segmentation capability of the FCM method on multispectral MRI images. The MFV is presented in Eq. 8.

$$WF = Wav\_Fusion(T1\_weighted, T2\_weighted, PD\_weighted) \tag{7}$$

$$MFV = [T1\_weighted(i, j), WF]^T \tag{8}$$

These three different feature vectors i.e., *F1, F2* and *MFV*, will be used in FCM method for multispectral MRI segmentation.

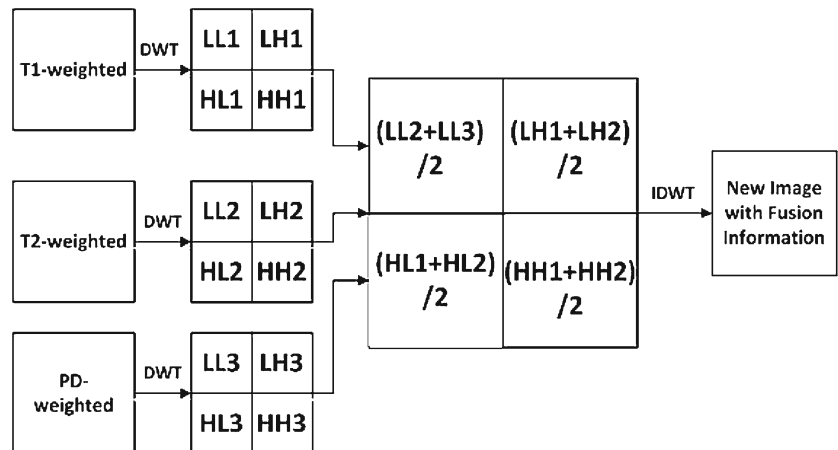
### 3.2 Combination of FCM clustering method and MRF model

Clustering methods such as finite mixture models (FMM) and FCM algorithms are commonly applied on brain image segmentation [12,17]. FCM algorithm is an iterative algorithm. Equation 9 is the objective function for FCM that has to be minimized.

$$J_m = \sum_{i=1}^N J_i = \sum_{i=1}^N \left( \sum_{j=1}^C u_{ij}^m \|x_i - c_j\|^2 \right), m \in R, m > 1 \tag{9}$$

where *N* is number of samples, *x* is *n*-dimensional sample and *C* is number of classes. *c<sub>j</sub>* is the *n*-dimensional center of the cluster *j*. Equations 10 and 11 show iterative steps to be followed to update different parameters such as center of the clusters and the degree of the class membership.

**Fig. 1** Proposed wavelet fusion method



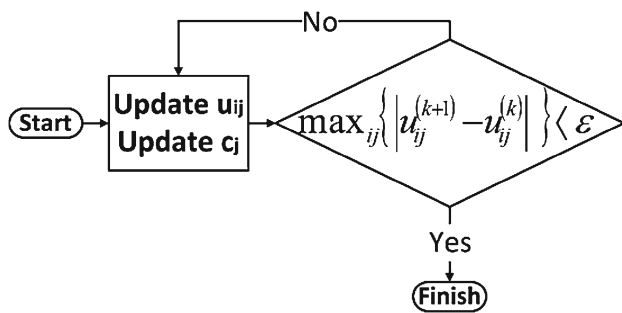


**Fig. 2** Flow chart for the iterative process of calculating the degree of the class membership ( $u_{ij}$ ) and center ( $c_j$ )

$$u_{ij} = 1 / \sum_{k=1}^C \left( \frac{\|x_i - c_j\|}{\|x_i - c_k\|} \right)^{\frac{2}{m-1}} \quad (10)$$

$$c_j = \sum_{i=1}^N u_{ij}^m \times x_i / \sum_{i=1}^N u_{ij}^m \quad (11)$$

where  $k$  is iteration number. Iteration stops when  $\max_{ij} \left\{ \left| u_{ij}^k - u_{ij}^{k-1} \right| \right\} < \varepsilon$ , where  $\varepsilon$  is a termination criterion between 0 and 1. Figure 2 shows a flow chart for the iterative process used for updating  $u_{ij}$  and  $c_j$ . MRF model is proposed by Besag [22]; however, this method was initially applied to the image processing area by Geman and Geman [23]. In this method, segmentation problem is turned into a labeling problem and goal is to find the best label field for all the segments. This method uses an energy function together with an optimization algorithm to minimize the energy function. This method uses EM for the parameter estimation and the simulated annealing to optimize the energy function.

MRF is one of the best methods for contextual image segmentation [8]. This method is applied on the neighborhood information in image segmentation. Conventional MRF method is very time-consuming. Combination of MRF and a typical clustering method was used to increase the robustness of the clustering method against the noise and reduce execution time for the MRF. Rajapakse et al. [12] used GMM for initial brain segmentation. Later on, MRF method was used to smooth different segments and to make the GMM more robust against noise.

Dubes et al. [11] also proposed a combination of clustering methods together with the MRF method to reduce computation burden and to increase robustness against noise. They used K-means clustering for the initial segmentation followed by the MRF method to increase the number of eliminated fragments in different segments. This method is proposed for one-dimensional image segmentation and Eq. 12 shows its energy function.

This energy functions consists of two parts, the first part includes cluster binding and the second part calculates neighboring energy for all the cliques in the image. The proposed

method uses only first part of the energy function in implementing the MRF method.  $E(y)$  is energy function used to incorporate spatial information in image segmentation for label field [11, 12].

$$U(y) = \frac{1}{2} \ln(\sigma_t^2) + \frac{(x - \mu_t)^2}{2\sigma_t^2} + E(y) \quad (12)$$

where  $U(y)$  is total energy of label field  $y$ .  $\mu_t$  and  $\sigma_t$  are mean and variance of segment  $t$ , respectively. Variable  $x$  stands for the pixel intensity.

### 3.3 Proposed method for multispectral MRI image segmentation

In this paper, two different methods are compared against each other. Each method follows a different approach in using spectral features in MRF. In the first method, different channels are segmented using FCM method. Here, a fuzzy segmentation is produced, and a membership degree is assigned to each pixel representing the membership of each pixel within a cluster. The highest class membership is used to select the class of each pixel.

Therefore, three different label fields are produced including  $T1$  label field,  $T2$  label field, and  $PD$  label field. The  $T1$  label field is used for the initial segmentation, and the other two label fields are used to incorporate spectral information in MRI segmentation. Neighborhood energy for this labeling is presented with  $V_{in-plane}$  ( $T1$  label field) and the other two label field as  $V_{out-plane}$ . Then, an energy function such as Eq. 12 is used in simulated annealing method for the optimization step. In this paper,  $E(y)$  is calculated using Eqs. 13 and 14.

$$E(y) = \sum_{c \in C} \left( \sum_{s=1}^8 V_{in-plan}(i, j) + 0.5 \times \sum_{s=1}^2 V_{out-plan}(i, k) \right), \quad i, j, k \in S \quad (13)$$

$$V_{in-plan} = V_{out-plan} = \begin{cases} -0.5 & \text{if } y_i = y_j \\ +0.5 & \text{if } y_i \neq y_j \end{cases}, \quad i, j \in S \quad (14)$$

where  $C$  presents the all possible cliques in the image and  $S$  is the lattice defined on the image. This work applies a new energy function for multispectral MRI image segmentation. In the proposed method, F1 and MFV vectors are segmented using FCM method and, consequently, two different label fields are produced. Like previous method  $T1$ -weighted label field is used as initial segmentation. Another label field that is produced by the MFV is used to incorporate spectral information in MRI image segmentation. According to Table 1, this label field has higher accuracy than other label fields such as

**Table 1** Dice index for different noise levels and three different INU levels

Feature vector	7%			
	CSF	GM	WM	Average
F1	91.60	84.13	80.97	86.79
F2	92.44	80.44	79.06	84.61
MFV	91.29	83.13	83.27	86.88
Feature vector	9%			
	CSF	CSF	CSF	Average
F1	88.37	79.40	77.00	82.81
F2	91.35	77.97	76.27	82.36
MFV	90.67	81.46	80.62	85.25

PD and T2 label fields. Therefore, the value of this label field has significant effect on the energy function. Neighborhood energy for T1 labeling is presented by  $V_{in-plane}$  and the other proposed label field by  $V_{out-plane}$ . In the proposed method,  $E(y)$  is presented by Eqs. 15 and 16 presents  $V_{in-plane}$  and  $V_{out-plane}$  values for different pixel locations.

$$E(y) = \sum_{c \in C} \left( 0.5 \times \left[ \sum_{s=1}^8 V_{in-plan}(i, j) \right] + 0.5 \times V_{out-plan}(i, k) \right), i, j, k \in S \quad (15)$$

$$V_{in-plan} = V_{out-plan} = \begin{cases} -1 & \text{if } y_i = y_j \\ +1 & \text{if } y_i \neq y_j \end{cases} i, j \in S \quad (16)$$

Flow chart of the proposed method for combining FCM with MFV and MRF method is presented in Fig. 3.

### 4 Experimental results

In the reported work, a well-known BrainWeb dataset that is captured at McConnell Brain Imaging Centre of the Mon-

treal Neurological Institute, McGill University [24], was used to evaluate the proposed method. Dice coefficient is used for comparison different feature vectors. Dice coefficient is described by Eq. 17.

$$D(k) = \frac{2 \times V_{p \cap g}(k)}{V_p(k) + V_g(k)} \quad (17)$$

In this equation,  $V_p(k)$  represents the proposed method of labeling for class  $k$ ,  $V_g(k)$  represents the ground truth labeling for class  $k$  and  $V_{p \cap g}(k)$  is the number of pixels with the same label in the proposed method and ground truth for class  $k$ . In other words, dice coefficient represents the overlap results of the aforementioned methods for the class  $k$ .

#### 4.1 Experiment 1

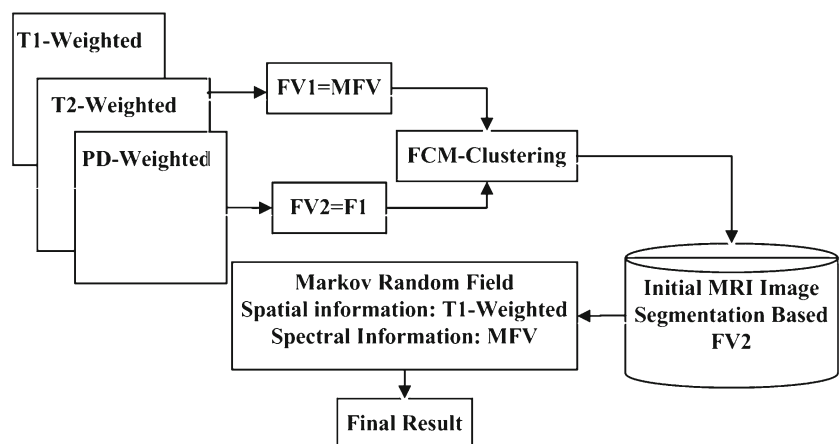
First experiment is aimed to compare three different feature vectors presented in Sect. 3.1. Table 1 shows average value of different INUs within each noise level. This experiment is performed on different INUs such as 0, 20, and 40% for two different high noise levels i.e., 7 and 9%.

Table 1 shows that the F2 feature vector has the worst average accuracy compared with other feature vectors, while the proposed feature vector has the best average accuracy. Daubechies 6-tap wavelet is used for the MFV feature vector extraction. Difference between values of MFV and F1 for 7% noise level is 0.09% while difference for 9% noise level is 2.44%. Therefore, results show that increasing noise level will increase effectiveness of the proposed method. Results for slices with 9% noise and 40% INU are presented in Fig. 4.

#### 4.2 Experiment 2

Experiment 2 compares two different MRF methods that are introduced in Sect. 3.2. Figure 5 depicts different segmentation results for MFV with FCM and the proposed energy function for MRF method. Figure 5 presents segmentation results for MRI images with 9% noise level and 40% INU.

**Fig. 3** Flow chart of the proposed method for multispectral MRI image with high level of noise





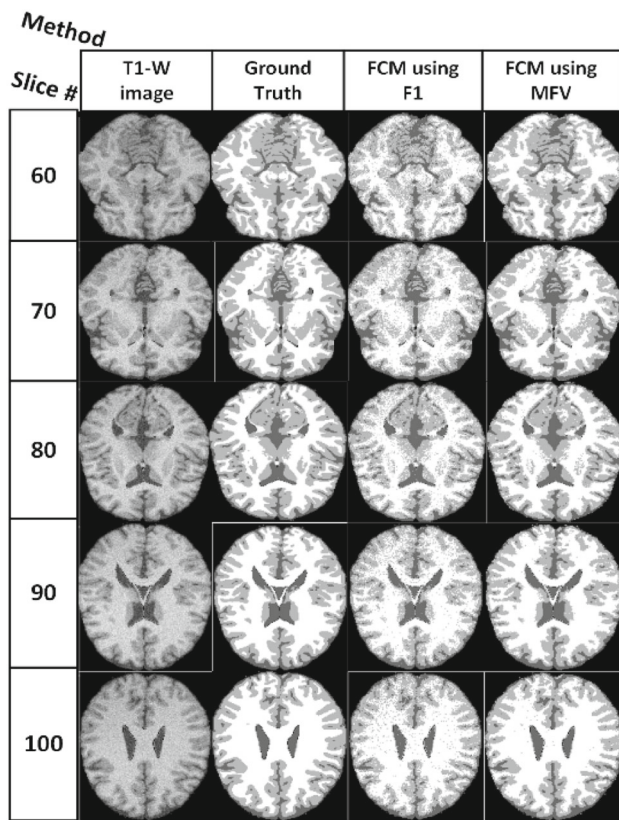


Fig. 4 Segmentation results for two different feature vectors

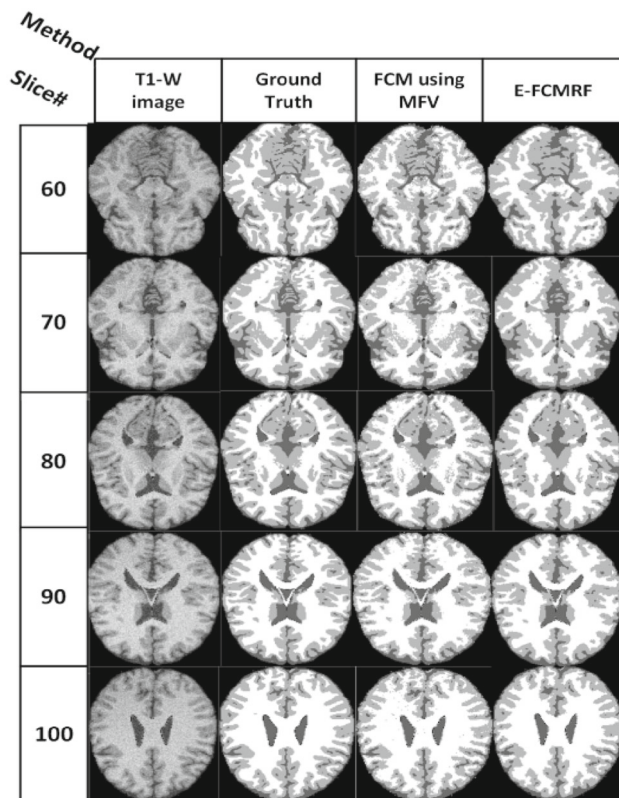


Fig. 5 Segmentation results for the two proposed methods

Table 2 Segmentation results for some slices

Slice number	CSF	GM	CSF	Average
<i>F1-FCM</i>				
40	88.56	79.53	73.86	79.98
50	85.37	81.69	65.73	79.97
60	80.26	82.10	81.51	81.67
70	87.59	80.94	82.93	82.71
80	87.71	83.10	84.35	84.29
90	88.47	81.44	88.45	85.86
100	87.63	82.80	90.55	87.42
110	86.67	84.53	89.78	87.24
120	89.92	84.61	86.51	86.25
130	92.22	81.33	86.35	85.87
Average	87.44	82.21	83.30	84.13
<i>MFV-FCM</i>				
40	86.12	80.96	80.73	81.98
50	82.55	80.72	69.18	79.31
60	81.92	88.99	90.12	88.43
70	87.50	86.92	94.23	89.92
80	85.77	88.01	94.26	89.98
90	87.14	85.89	98.20	92.02
100	89.15	86.34	98.22	92.85
110	89.42	87.58	97.25	92.33
120	92.98	88.57	92.54	90.79
130	95.46	85.59	92.96	90.72
Average	87.80	85.97	90.76	88.83
<i>Proposed method</i>				
40	92.65	89.54	86.06	89.32
50	89.00	90.61	80.83	88.77
60	85.20	89.63	89.59	89.04
70	90.38	88.19	89.90	89.20
80	89.82	89.09	90.41	89.70
90	91.36	87.82	92.64	90.67
100	89.94	88.53	94.12	91.60
110	88.85	89.86	93.71	91.54
120	91.18	89.35	91.03	90.28
130	93.75	86.80	90.56	89.90
Average	90.21	88.94	89.88	90.02

A detailed comparison between different slices is presented in Table 2. Table 2 presents dice coefficient for different segments for 9% noise and 40% INU.

Figure 6a depicts dice coefficient for different iterations calculated for the slice 80 with 9% noise and 40% INU using the proposed method. Figure 6b depicts averaged dice coefficient for different iterations calculated for all of the slices, with 9% noise and 40% INU using the proposed method. Figure 6a, b show that during early iterations, the accuracy increases quickly. However, after a while, its rate is decreased.

**Fig. 6** **a** Accuracy in different iterations. **b** Averaged accuracy in different iterations

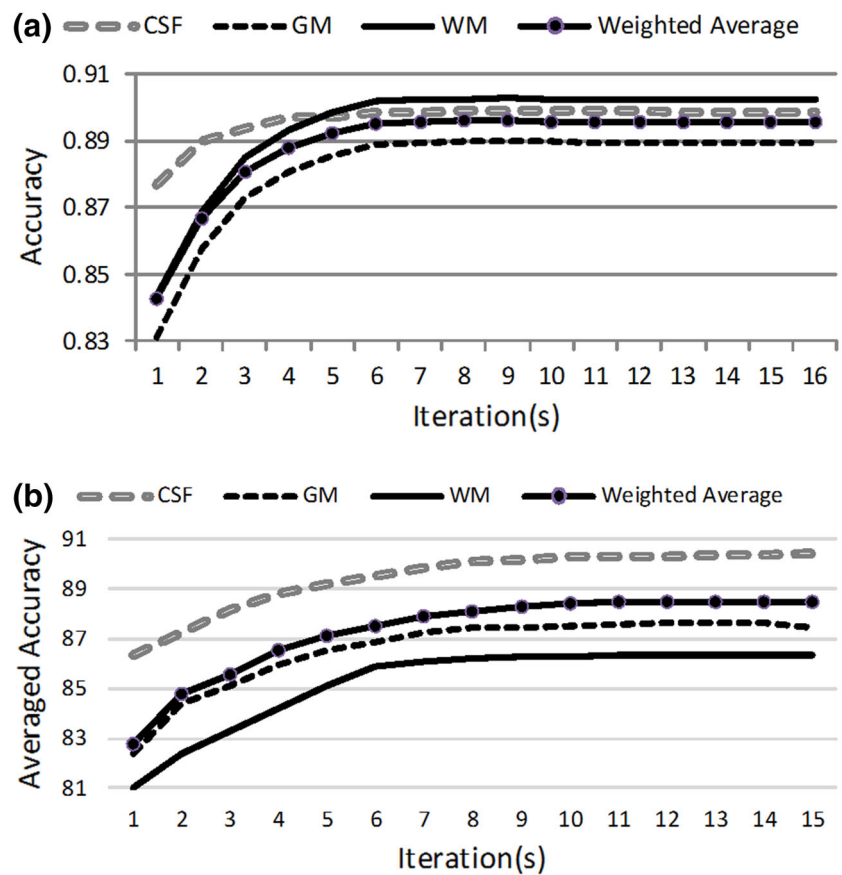


**Table 3** Dice index for different noise levels and three different INU levels for proposed MRF method

Method	CSF	GM	WM	Average
<i>7% noise</i>				
FCM using F1	91.16	84.13	80.97	86.79
FCM using MFV	91.29	83.13	83.27	86.88
FCMRF	92.46	87.21	85.63	89.78
E-FCMRF	92.66	89.53	88.12	90.14
GMM-GA	90.41	86.08	82.94	87.81
KVL	–	89.54	89.30	89.38
MPM-MAP	–	91.75	90.57	91.16
<i>9% noise</i>				
FCM using F1	88.37	79.40	77.00	82.81
FCM using MFV	90.67	81.46	80.62	85.25
FCMRF	90.93	85.26	84.00	88.11
E-FCMRF	91.42	87.64	86.37	88.52
GMM-GA	87.97	82.14	78.66	83.69
KVL	–	87.45	87.10	87.40
MPM-MAP	–	89.50	88.15	88.79

Figure 6a shows that WM has better segmentation accuracy in comparison with other segments. Figure 6b shows that WM has the lowest segmentation accuracy. This effect

is due to low volume of WM in initial and final slices of the brain. This is why the WM segmentation of these slices produces a bad segmentation result. Therefore, average measure on all of the slices resulted in low segmentation accuracy in comparison with the results from each individual segment.

Using finite mixture models, researchers have reported excellent results in MRI brain segmentation. Ferreira da Silva [25] compared three effective and well-known methods such as MPM-MAP [13], KVL [9], and EM-HMRF [14] against the reported method that is called Dirichlet Process Mixture Model (DPMM). Results show that MPM-MAP outperforms other methods. Hence, it was decided to use experimental results out of KVL, MPM-MAP, and GMM-GA [7] for the evaluation purpose. GMM-GA method is applied on LONI (Library of Neuro Imaging) software from university of UCLA [26], for the evaluation of the proposed method. Reason for selecting these three methods is their similar approach for segmentation, accuracy, and their popularity. Intension was to compare the proposed method against strong competitors. Experimental results show that applying the proposed method for multispectral image segmentation in two different high noise levels will produce better accuracy compared with FCMRF and GMM-GA. Experimental results are compared versus two well-known and effective methods such as KVL and MPM-MAP. Detection accura-

cies for seven different methods are presented in two different noise levels of 7 and 9% in Table 3.

In Table 3, weighted average of other three columns i.e., CSF, GM, and WM is reported in a column labeled “Average”. Each one of the CSF, GM, and WM values are corresponding average values on three INU levels i.e., 0, 20, and 40. Comparing the proposed method against KVL, the proposed method provides better weighted average accuracy. The accuracy of the proposed method is less than MPM-MAP; however, their difference is small.

## 5 Conclusions and future work

This paper proposes a new data fusion method for multispectral MRI image segmentation on noisy MRI images.

Different feature vectors are used for comparison in high noise levels. FCM method is applied on different feature vectors. The reported results show that MFV produces promising result against noise. This paper also proposes a new method based on the use of a combination of FCM and MRF methods. MFV is used to incorporate spectral information in the optimization step. Results show that the proposed method has a good immunity against noise and different artifacts such as INU. Results also show that in comparison with the other well-known methods such as GMM-GA, FCM, and FCMRF the proposed method provides better segmentation accuracy for different tissues. The proposed method uses simulated annealing as for the optimization step; therefore, it has high computational complexity and is slow. Improvement of the execution time is a research necessity that is left for the future work.

## References

- Lin, G.C., Wang, W.J., Kang, C.C., Wang, C.M.: Multispectral MR images segmentation based on fuzzy knowledge and modified seeded region growing. *Magn. Reson. Imaging* **30**(2), 230–246 (2012)
- Yousefi, S., Azmi, R., Zahedi, M.: Brain tissue segmentation in MR images based on a hybrid of MRF and social algorithms. *Med. Image Anal.* **16**(4), 840–848 (2012)
- Ghasemi, J., Ghaderi, R., Karami Mollaei, M., Hojjatoleslami, S.: A novel fuzzy Dempster–Shafer inference system for brain MRI segmentation. *Inf. Sci.* **223**, 205–220 (2013)
- Szilágyi, L., Szilágyi, S.M., Benyó, B.: Efficient inhomogeneity compensation using fuzzy C-means clustering models. *Comput. Methods Prog. Biomed.* **108**(1), 80–89 (2012)
- Greenspan, H., Ruf, A., Goldberger, J.: Constrained Gaussian mixture model framework for automatic segmentation of MR brain images. *IEEE Trans. Med. Imaging* **25**(9), 1233–1245 (2006)
- Tohka, J., Krestyannikov, E., Dinov, I., Shattuck, D., Ruotsalainen, U., Toga, A.: Genetic algorithms for finite mixture model based tissue classification in brain MRI. In: Proceedings of the European Medical and Biological Engineering Conference (IFMBE), pp. 4077–4082 (2005)
- Tohka, J., Krestyannikov, E., Dinov, I.D., Graham, A., Shattuck, D.W., Ruotsalainen, U., Toga, A.W.: Genetic algorithms for finite mixture model based voxel classification in neuroimaging. *IEEE Trans. Med. Imaging* **26**(5), 696–711 (2007)
- Dey, V., Zhang, Y., Zhong, M.: A review on image segmentation techniques with remote sensing perspective. In: Proceedings of the International Society for Photogrammetry and Remote Sensing Symposium (ISPRS10), Vienna, pp. 5–7 (2010)
- Van Leemput, K., Maes, F., Vandermeulen, D., Suetens, P.: Automated model-based tissue classification of MR images of the brain. *IEEE Trans. Med. Imaging* **18**(10), 897–908 (1999)
- Balafar, M.: Gaussian mixture model based segmentation methods for brain MRI images. *Artif. Intell. Rev.* **41**(3), 1–11 (2012)
- Dubes, R., Jain, A., Nadabar, S., Chen, C.: MRF model-based algorithms for image segmentation. In: Proceedings of the 10th International Conference Pattern Recognition, pp. 808–814 (1990)
- Rajakpake, J.C., Giedd, J.N., Rapoport, J.L.: Statistical approach to segmentation of single-channel cerebral MR images. *IEEE Trans. Med. Imaging* **16**(2), 176–186 (1997)
- Marroquín, J.L., Vemuri, B.C., Botello, S., Calderon, E., Fernandez-Bouzas, A.: An accurate and efficient Bayesian method for automatic segmentation of brain MRI. *IEEE Trans. Med. Imaging* **21**(8), 934–945 (2002)
- Zhang, Y., Brady, M., Smith, S.: Segmentation of brain MR images through a hidden Markov random field model and the expectation-maximization algorithm. *IEEE Trans. Med. Imaging* **20**(1), 45–57 (2001)
- Pham, D., Prince, J.L., Xu, C., Dagher, A.P.: An automated technique for statistical characterization of brain tissues in magnetic resonance imaging. *Int. J. Pattern Recognit. Artif. Intell.* **11**(08), 1189–1211 (1997)
- Caldairou, B., Passat, N., Habas, P.A., Studholme, C., Rousseau, F.: A non-local fuzzy segmentation method: application to brain MRI. *Pattern Recognit.* **44**(9), 1916–1927 (2011)
- Rivest-Hénault, D., Chériet, M.: Unsupervised MRI segmentation of brain tissues using a local linear model and level set. *Magn. Reson. Imaging* **29**(2), 243–259 (2011)
- Wu, T., Bae, M.H., Zhang, M., Pan, R., Badea, A.: A prior feature SVM-MRF based method for mouse brain segmentation. *NeuroImage* **59**(3), 2298–2306 (2012)
- Riklin-Raviv, T., Van Leemput, K., Menze, B.H., Wells III, W.M., Golland, P.: Segmentation of image ensembles via latent atlases. *Med. Image Anal.* **14**(5), 654–665 (2010)
- Wang, Z., Ziou, D., Armenakis, C., Li, D., Li, Q.: A comparative analysis of image fusion methods. *IEEE Trans. Geosci. Remote Sens.* **43**(6), 1391–1402 (2005)
- Nunez, J., Otazu, X., Fors, O., Prades, A., Pala, V., Arbiol, R.: Multiresolution-based image fusion with additive wavelet decomposition. *IEEE Trans. Geosci. Remote Sens.* **37**(3), 1204–1211 (1999)
- Besag, J.: Statistical analysis of non-lattice data. *Statistician* **24**(3), 179–195 (1975)
- Geman, S., Geman, D.: Stochastic relaxation, Gibbs distributions, and the Bayesian restoration of images. *IEEE Trans. Pattern Anal. Mach. Intell.* **6**(6), 721–741 (1984)
- Collins, D.L., Zijdenbos, A.P., Kollokian, V., Sled, J.G., Kabani, N.J., Holmes, C.J., Evans, A.C.: Design and construction of a realistic digital brain phantom. *IEEE Trans. Med. Imaging* **17**(3), 463–468 (1998)
- Ferreira da Silva, A.R.: A Dirichlet process mixture model for brain MRI tissue classification. *Med. Image Anal.* **11**(2), 169–182 (2007)
- The homepage for the LONI (“Laboratory of Neuro Imaging”) software package, <http://www.loni.usc.edu/Software/>, as visited on 2014